

Controlled Self-Assembly of Monodisperse Niosomes by Microfluidic Hydrodynamic Focusing

Catherine T. Lo,[†] Andreas Jahn,^{‡,§} Laurie E. Locascio,[†] and Wyatt N. Vreeland^{*,†}

[†]Biochemical Science Division, National Institute of Standards and Technology, 100 Bureau Drive, Gaithersburg, Maryland 20899, and [‡]Semiconductor Electronics Division, National Institute of Standards and Technology, 100 Bureau Drive, Gaithersburg, Maryland 20899. [§]Currently at Laboratory of Organic Chemistry, ETH Zürich, Wolfgang-Pauli-Strasse 10, 8093 Zürich, Switzerland.

Received December 8, 2009. Revised Manuscript Received January 21, 2010

Niosomes are synthetic membrane vesicles formed by self-assembly of nonionic surfactant, often in a mixture with cholesterol and dicetyl phosphate. Because of their inner aqueous core and bilayer membrane shell, niosomes are commonly used as carriers of treatment agents for pharmaceutical and cosmetic applications or contrast agents for clinical imaging applications. In those applications, niosomes are considered as a more economical and stable alternative to their biological counterpart (i.e., liposomes). However, conventional bulk method of niosome preparation requires bulk mixing of two liquid phases, which is time-consuming and not well-controlled. Such mixing conditions often lead to large niosomes with high polydispersity in size and thus affect the consistency of niosome dosage or imaging quality. In this study, we present a new method of niosome self-assembly by microfluidic hydrodynamic focusing to improve on the size and size distributions of niosomes. By taking advantage of the rapid and controlled mixing of two *miscible* fluids (i.e., alcohol and water) in microchannels, we were able to obtain in seconds nanoscaled niosomes with $\approx 40\%$ narrower size distributions compared to the bulk method. We further investigated different parameters that might affect on-chip assembly of niosomes, such as (1) conditions for the microfluidic mixing, (2) chemical structures of the surfactant used (i.e., sorbitan esters Span 20, Span 60, and Span 80), and (3) device materials for the microchannel fabrication. This work suggests that microfluidics may facilitate the development and optimization of biomimetic colloidal systems for nanomedicine applications.

1. Introduction

Niosomes are synthetic membrane vesicles made by self-assembly of nonionic surfactants (i.e., amphiphilic compounds that do not dissociate at neutral pH). They are often composed of nonionic surfactant, cholesterol, and dicetyl phosphate, in molar ratios of 47.5:47.5:5.0, respectively.^{1–3} Their structure and properties are similar to those of their biological counterpart (i.e., liposomes), which are membrane vesicles composed of biological phospholipids. Niosomes can encapsulate hydrophilic molecules in their inner aqueous core and partition hydrophobic ones into their bilayer membrane.^{4,5} They are commonly used as carriers of treatment agents and can also be surface modified to target specific tissues for localized delivery.^{6–8} Because of their relative low cost and chemical stability, niosomes are considered an attractive alternative to liposomes in the pharmaceutical and cosmetic industries.^{4,5} Niosomes were initially developed and patented by the cosmetic company L’Oreal in the late 1970s, and the first commercial product of “Niosome” antiaging cream

was introduced to the market in the 1980s. It was reported that the advantages of using niosomes in cosmetic applications include their ability to stabilize the encapsulated treatment agents, improve bioavailability of such agents, and enhance skin absorption of such agents.⁹ Since then, niosomes have also been evaluated in pharmaceutical applications, such as delivery of anticancer drugs (e.g., doxorubicin and paclitaxel) and anti-inflammatory drugs (e.g., rifampicin and flurbiprofen).^{10–13} In such therapeutic applications, important advantages of using niosomes include their ability to reduce systemic toxicity by encapsulation of treatment agents and minimize clearance of such agents from the body by slow drug release.^{3–5} In recent years, niosomes have also been used as carriers of contrast agents for targeted, clinical imaging applications for more accurate medical diagnosis.^{14,15}

Conventional bulk methods for niosome preparation in the laboratory (e.g., film hydration or alcohol injection) are performed by mixing two liquid phases in beakers or test tubes for their spontaneous self-assembly into niosomes.^{4,5} In such bulk mixing, however, the local chemical and mechanical environments are not well-controlled and often result in niosomes with

*Corresponding author: Tel (301) 975-8513; e-mail wyatt.vreeland@nist.gov.

(1) Baillie, A. J.; Florence, A. T.; Hume, L. R.; Muirhead, G. T.; Rogerson, A. *J. Pharm. Pharmacol.* **1985**, *37*, 863.

(2) Yoshioka, T.; Sternberg, B.; Florence, A. T. *Int. J. Pharm.* **1994**, *105*, 1.

(3) Uchegbu, I. F.; Vyas, S. P. *Int. J. Pharm.* **1998**, *172*, 33.

(4) Uchegbu, I. F. *Synthetic Surfactant Vesicles: Niosomes and Other Non-Phospholipid Vesicular Systems*, 1st ed.; CRC: Boca Raton, FL, 2000; p 93.

(5) Sahin, N. O. In *Nanomaterials and Nanosystems for Biomedical Applications*; Mozafari, M. R., Ed.; Springer: Berlin, 2007; p 67.

(6) Dufes, C.; Gaillard, F.; Uchegbu, I. F.; Schatzlein, A. G.; Olivier, J. C.; Muller, J. M. *Int. J. Pharm.* **2004**, *285*, 77.

(7) Azeem, A.; Anwer, M. K.; Talegaonkar, S. *J. Drug Targeting* **2009**, *17*, 671.

(8) Hong, M.; Zhu, S.; Jiang, Y.; Tang, G.; Pei, Y. *J. Controlled Release* **2009**, *133*, 96.

(9) Handjani-Vila, R. M.; Ribier, A.; Rondot, B.; Vanlerberghie, G. *Int. J. Cosmet. Sci.* **1979**, *1*, 303.

(10) Jain, C. P.; Vyas, S. P. *J. Microencapsulation* **1995**, *12*, 401.

(11) Uchegbu, I. F.; Double, J. A.; Kelland, L. R.; Turton, J. A.; Florence, A. T. *J. Drug Targeting* **1996**, *3*, 399.

(12) Mokhtar, M.; Samsour, O. A.; Hammad, M. A.; Megrab, N. A. *Int. J. Pharm.* **2008**, *361*, 104.

(13) Bayindir, Z. S.; Yuksel, N. *J. Pharm. Sci.* **2010**, *99*, 2049.

(14) Müller, D.; Foulon, M.; Bonnemain, B.; Vandamme, T. F. *J. Microencapsulation* **2000**, *17*, 227.

(15) Luciani, A.; Olivier, J. C.; Clement, O.; Siauve, N.; Brillet, P. Y.; Bessoud, B.; Gazeau, F.; Uchegbu, I. F.; Kahn, E.; Frija, G.; Cuenod, C. A. *Radiology* **2004**, *231*, 135.

high polydispersity in size.^{4,5} Additional size-altering postprocessing steps, such as extrusion or sonication, are required to obtain smaller and more homogeneous niosome population. The ability to control niosome size and size distribution during production is a critical factor in determining the success of the niosome system *in vivo*, as the size of niosomes influence their circulation time in the body and can affect niosome dosage or imaging quality. Generally, nanoparticles < 10 nm in diameter are cleared by the renal system more rapidly than larger ones.¹⁶ However, larger nanoparticles also have greater surface areas, which can accommodate higher number of surface recognitions sites and thus increase their chance of recognition and clearance by the complementary systems (i.e., macrophage phagocytosis).¹⁷ The liver can also capture and eliminate nanoparticles > 100 nm in diameter.¹⁶ Since niosomes are a type of nanoparticle, they should ideally be > 10 nm and < 100 nm in diameter and monodisperse in size distribution to be utilized in clinical applications. That particular size range is optimal for minimal clearance from the body, and the monodisperse size population is more consistent in encapsulation of molecules for more reliable clinical therapeutics and imaging.

Our group was the first to report on the rapid and highly efficient microfluidic hydrodynamic focusing for the controlled self-assembly of monodisperse liposomes.^{18,19} Mechanistically, a central stream containing the lipid mixture in isopropyl alcohol was introduced to two adjacent phosphate buffer streams flowing at higher flow rates. At low Reynolds numbers, the central stream was focused into a narrow stream, and the width of the focused stream then enabled rapid mixing of the two fluids through diffusion. This method is not to be confused with the droplet formation process in other microfluidic systems, in which microscaled droplets are formed based on the interfacial tension between two *immiscible* fluids.^{20–22} In our system, nanoscaled liposomes are formed by the diffusive mixing at the interface between two *miscible* phases (i.e., alcohol and water). We anticipate that monodisperse niosomes can be rapidly assembled by such diffusive mixing, using microfluidic hydrodynamic focusing (Figure 1). Assuming that the fluid flow profile is not significantly altered by the difference in viscosity between the focused alcohol stream and the buffer streams and that the majority of diffuse mixing occurs after the three fluid streams have converged, the diffusive mixing time (τ_{mix}) for niosome self-assembly can be estimated using a simple two-dimensional model.²³

$$\tau_{\text{mix}} \sim \frac{w_f^2}{4D} \approx \frac{w^2}{9D(1+\text{FRR})^2} \quad (1)$$

where D is the diffusivity of the solvent, w_f is the width of the focused stream, w is the microchannel width, and FRR is the flow rate ratio of phosphate buffer to isopropyl alcohol.

The main objective of this work was to investigate parameters that might affect on-chip assembly of niosomes, such as (1) conditions for the diffusive mixing, (2) chemical structures of

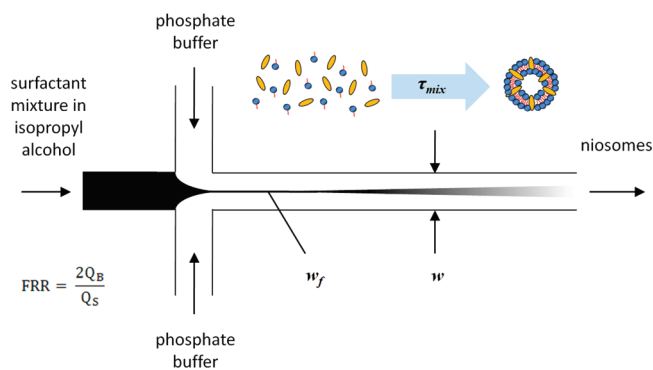


Figure 1. Schematics of niosome self-assembly by microfluidic hydrodynamic focusing. A central stream containing the surfactant mixture (i.e., sorbitan ester, cholesterol, and dicetyl phosphate) in isopropyl alcohol is focused by adjacent streams of phosphate buffer in a microfluidic format. Flow rate ratio (FRR) is defined as the ratio of the buffer volumetric flow rates (Q_B) to the alcohol volumetric flow rate (Q_S). The width of the focusing stream (w_f) enables rapid and controlled mixing of the two *miscible* fluids (i.e., alcohol and water) through diffusion, which facilitates on-chip assembly of niosomes. The diffusive mixing time (τ_{mix}) can be estimated by eq 1.

the surfactant used, and (3) device materials for the microchannel fabrication. Sorbitan esters were selected as the surfactant to test in this study because they are FDA approved for use in food processing and pharmaceuticals^{24,25} and have been previously identified as a suitable surfactant for preparing niosomes.^{2,26} They are safe, amphiphilic compounds derived from sorbitol (i.e., a synthetic sweetener). Compared with biological phosphatidylcholines that are typically used in liposome preparation, synthetic sorbitan esters are much less expensive: 1 g of phosphatidylcholines, for example, costs the same as 1000 g of sorbitan esters. Three different sorbitan esters were evaluated for the affect of alkyl chain length and presence of an unsaturated double bond on the properties of the assembled niosomes. Additionally, niosome self-assembly using microfluidic hydrodynamic focusing was examined in both the silicon metal microchannels and the PDMS polymer microchannels, which are more accessible to biological laboratories (i.e., without a need of a cleanroom setting). This work suggests that microfluidics may facilitate the development and optimization of biomimetic colloidal systems for nanomedicine applications.

2. Experimental Section²⁷

Silicon Device Fabrication. A silicon device was fabricated as previously described.^{18,19} Briefly, microchannels were patterned and etched into the front side of a silicon wafer using standard photolithographic and deep reactive ion etching (DRIE) processes. Access holes were then patterned and etched through the backside of the wafer by DRIE at each channel terminus. The final device was sealed by anodic bonding of the silicon wafer to a borosilicate glass wafer. Cross-section dimensions of the main focusing channel in the silicon device were 65 μm wide \times 120 μm

(16) Gullotti, E.; Yeo, Y. *Mol. Pharmaceutics* **2009**, *6*, 1041.
 (17) Ishida, T.; Harashima, H.; Kiwada, H. *Biosci. Rep.* **2002**, *22*, 197.
 (18) Jahn, A.; Vreeland, W. N.; Gaitan, M.; Locascio, L. E. *J. Am. Chem. Soc.* **2004**, *126*, 2674.
 (19) Jahn, A.; Vreeland, W. N.; DeVoe, D. L.; Locascio, L. E.; Gaitan, M. *Langmuir* **2007**, *23*, 6289.
 (20) Thorsen, T.; Roberts, R. W.; Arnold, F. H.; Quake, S. R. *Phys. Rev. Lett.* **2001**, *86*, 4163.
 (21) Anna, S. L.; Bontoux, N.; Stone, H. A. *Appl. Phys. Lett.* **2003**, *82*, 364.
 (22) Link, D. R.; Anna, S. L.; Weitz, D. A.; Stone, H. A. *Phys. Rev. Lett.* **2004**, *92*, 054503.
 (23) Karnik, R.; Gu, F.; Basto, P.; Cannizzaro, C.; Dean, L.; Kyei-Manu, W.; Langer, R.; Farokhzad, O. C. *Nano Lett.* **2008**, *8*, 2906.

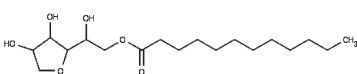
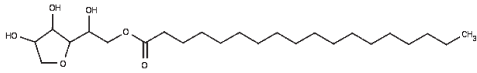
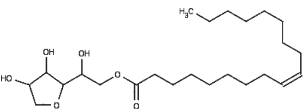
(24) Cottrell, T.; van Peij, J. In *Emulsifiers in Food Technology*; Whitehurst, R. J., Ed.; Blackwell Publishing Ltd.: Oxford, 2004; p 162.

(25) Sweetman, S. C. *Martindale: The Complete Drug Reference*, 36th ed.; Pharmaceutical Press: London, 2009; p 3694.

(26) Chandraprakash, K. S.; Udupa, N.; Umadevi, P.; Pillai, G. K. *Int. J. Pharm.* **1990**, *61*, R1.

(27) Certain commercial equipment, instruments, or materials are identified in this report to specify adequately the experimental procedures only. Such identification does not imply a recommendation or endorsement by the National Institute of Standards and Technology, nor does it imply that the materials or equipment identified are necessarily the best available for the purpose.

Table 1. Properties of Selected Sorbitan Esters

Compound Name	Chemical Structure	Alkyl Chain Length	Transition Temperature (T_c)
Sorbitan Monolaurate (Span 20)		C ₁₂	liquid at 25 °C
Sorbitan Monostearate (Span 60)		C ₁₈	45 °C ^{2, 29}
Sorbitan Monooleate (Span 80)		C ₁₈	-30 °C ³⁰

high. The total length of the mixing region in the microchannel was 1 cm. Nanopore fluidic connectors (Upchurch Scientific, Oak Harbor, WA) were adhered to the backside of the silicon wafer to interface each channel access hole to standard syringe pumps (Harvard Apparatus, Holliston, MA) with poly(ether ether ketone) (PEEK) capillary tubings. Solutions that are needed to make the niosomes were introduced into the central microchannel by using a 500 μ L gastight glass syringe (Hamilton, Reno, NV) and into the side channels with 3 mL plastic syringes (BD, Franklin Lakes, NJ).

PDMS Device Casting. PDMS and its curing agent (Sylgard 184, Dow Corning, Midland, MI) were mixed at 10:1 ratio for 5 min. The PDMS solution was degassed, poured over the master template, cured at 80 °C for 2 h, and pulled from the template. The cured PDMS was sealed to a 1 mm thick microscope glass slide using a home-built microwave oxygen plasma system.²⁸ Briefly, the PDMS was placed with the glass slide into a glass desiccator, with a piece of aluminum foil covering the bottom. A vacuum was pulled for 60 s to purge the desiccator of oxygen (pressure reduced to 133 Pa). The desiccator and its contents were then placed into a conventional domestic microwave oven (Panasonic NN-S949BA) for plasma treatment by microwaves at 360 W for 10 s. The PDMS/glass was left in an 80 °C oven for an additional 2 h to enhance the plasma bonding. The dimensions of the main focusing channel in the glass-bonded PDMS device were 400 μ m wide \times 56 μ m high \times 3 cm long. Access holes were punched at the channel termini for insertion of Tygon tubing to connect standard syringe pumps (Harvard Apparatus, Holliston, MA) to the PDMS device for pressure-driven flow. Solutions that are needed to make the niosomes were introduced into the microchannels in the exact same manner as the silicon device.

Surfactant Mixtures and Hydration Buffer. Three different sorbitan esters were used in this study as shown in Table 1. Sorbitan monolaurate (Span 20: $\geq 44\%$ lauric acid, balance is primarily myristic, palmitic, and linolenic acids), sorbitan monostearate (Span 60: $\approx 50\%$ stearic acid, balance is primarily palmitic acid), and sorbitan monooleate (Span 80: $\geq 60.0\%$ oleic acid, balance is primarily linoleic, linolenic, and palmitic acids) were purchased from Sigma-Aldrich (St. Louis, MO). Phosphate buffered saline packets (PBS) were also purchased from Sigma. Cholesterol was purchased from Avanti Polar Lipids (Alabaster, AL). Dicetyl phosphate (DCP) was purchased from M.P. Biomedicals (Solon, OH). Chloroform and isopropyl alcohol (IPA) were obtained from J.T. Baker (Phillipsburg, NJ).

Span, cholesterol, and DCP were dissolved in chloroform and prepared in a molar ratio of 47.5:47.5:5.0, respectively, at a total of 10 mg/mL in a glass scintillation vial. The chloroform solvent was evaporated under nitrogen gas to form a dry surfactant film on the

bottom of the scintillation vial. The vial was then placed into a vacuum desiccator for at least 24 h to ensure complete solvent removal. The dried surfactant mixture was resolubilized in IPA at 5 mmol/L concentration. PBS (10 mmol/L phosphate, 2.7 mmol/L potassium chloride, 138 mmol/L NaCl, and pH 7.4, with 200 ppm sodium azide) was used as the hydration buffer for the niosome self-assembly in the microfluidic devices.

Rapid On-Chip Assembly of Niosomes. Niosomes were assembled on-chip by injecting the surfactant mixture, resolubilized in IPA, into the central microchannel. The surfactant/IPA stream was then hydrodynamically focused by two adjacent streams of PBS. The flow rate ratio (FRR), defined as the ratio of the PBS volumetric flow rate (Q_B) to the IPA volumetric flow rate (Q_S), was varied from 15 to 50. The total volumetric flow rate (Q_T) was maintained at a constant flow among all FRRs in the microchannel. Niosome self-assembly at different Q_T was also investigated at 50 and 100 μ L/min for the silicon device. For the PDMS device, Q_T at 125 μ L/min was investigated, which maintained the same volumetric flux as the 50 μ L/min flow rate in the silicon device.

$$\text{FRR} = \frac{2Q_B}{Q_S} \quad (2a)$$

$$Q_T = 2Q_B + Q_S \quad (2b)$$

The stability of the focusing region in the silicon device was observed at 20 \times magnification, under a Carl Zeiss Axioplan 2 microscope (Thornwood, NY), and captured by a Hamamatsu CCD digital camera (Bridgewater, NJ). Focusing in the PDMS device was observed under a Olympus MVX10 stereoscope (Westmont, IL) at 40 \times magnification and captured by a Nikon CoolPix 8800 VR digital camera (Melville, NY). Span 20, Span 60, and Span 80 mixtures in IPA were investigated for niosome self-assembly in the microfluidic devices.

High-Resolution Niosome Size Measurement. Niosomes prepared by the microfluidic method were collected and analyzed off-chip for their average sizes and size distributions. Size-based separation of niosome population was carried out using asymmetric flow-field flow fractionation (AF⁴), in conjunction with multiangle laser light scattering (MALLS) characterization (model DAWN EOS, Wyatt Technology, Santa Barbara, CA). The general principle of AF⁴ is to apply a high cross-flow to initially focus niosomes against a membrane, and then a quasi-parabolic flow is applied perpendicularly to elute niosomes with regard to size: smaller niosomes will elute before larger ones.

A cross-flow of 2 mL/min was ramped down linearly to 0 mL/min over 90 min, with an elution flow of 1 mL/min to separate the niosomes. A maximum sample volume of 100 μ L was injected for fractionation to minimize membrane overloading. Each fractionated sample was monitored by the MALLS detector during the

(28) Kralj, J. G.; Player, A.; Sedrick, H.; Munson, M. S.; Petersen, D.; Forry, S. P.; Meltzer, P.; Kawasaki, E.; Locascio, L. E. *Lab Chip* **2009**, 9, 917.

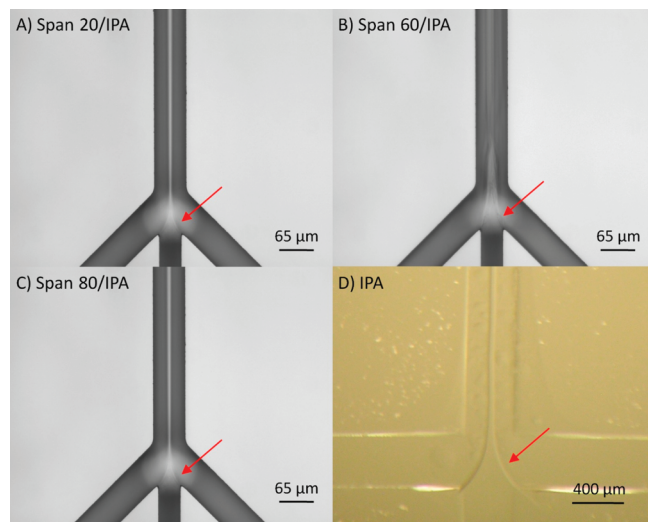


Figure 2. Microfluidic hydrodynamic focusing of a central stream containing either (A) Span 20/IPA, (B) Span 60/IPA, or (C) Span 80/IPA mixture by two adjacent PBS streams was visualized in the silicon device. Main microchannel dimensions were $65\ \mu\text{m}$ wide \times $120\ \mu\text{m}$ high. (D) Similar focusing was achieved in the PDMS microchannel with $400\ \mu\text{m}$ width \times $56\ \mu\text{m}$ height. Arrows denote the focusing regions. Note that the hydrodynamic focusing of Span 60/IPA was unstable, putatively due to aggregates not visible in the micrograph. All images were taken at the lowest FRR of 15.

elution process, and the radii of the eluted niosomes were calculated by fitting the angular scattering function to the Berry model in Astra V software (Wyatt Technology). Postpreparation, time-dependent stability of niosome size was evaluated over a course of 2 weeks, with the niosomes collected from the silicon device at $Q_T = 100\ \mu\text{L}/\text{min}$. Niosomes were stored at $25\ ^\circ\text{C}$ and analyzed on the day they were prepared, after 7 days, and after 14 days.

Confirmation of Self-Assembled Membranes. Niosomes collected from the PDMS device at the lowest FRR of 15 were stained with an intercalating dye to confirm the presence of self-assembled membranes. The lipophilic carbocyanine dye, DiIC₁₈-(3), was purchased from Invitrogen (Carlsbad, CA) and prepared at $1\ \mu\text{mol}/\text{L}$ concentration for staining of the niosomes. The quantum yield of this lipophilic dye increases dramatically once it intercalates into an intact membrane; the fluorescence background of the dye dissolved in water is minimal. Staining conditions were at $25\ ^\circ\text{C}$ for 1 h, at a 1:1 dilution of the niosome sample to the dye solution. The stained niosome sample was visualized using fluorescence microscopy (Carl Zeiss Observer Z.1, Thornwood, NY), with a rhodamine filter (545 nm excitation) at $10\times$ magnification. Fluorescence images were captured by a Hamamatsu EMCCD digital camera (Bridgewater, NJ).

3. Results and Discussion

T_c Affects Hydrodynamic Focusing of Surfactant Mixtures. Microfluidic hydrodynamic focusing of various surfactant mixtures resolubilized in IPA (i.e., Span 20/IPA, Span 60/IPA, and Span 80/IPA) was investigated in the silicon device. The focusing region for each niosome mixture at the lowest FRR of 15 is shown in Figure 2A–C. Mixtures with Span 20 and Span 80 had clearly visible, sharply focused streams of surfactant/IPA, while the mixture with Span 60 resulted in an unstable, fluctuating focusing. This phenomenon can be explained by the differences in the transition temperatures (T_c) among the Spans. Both Span 20 and Span 80 are stable liquids at $25\ ^\circ\text{C}$; thus, they were stable after contact with PBS during the focusing. Span 60, in contrast, is a

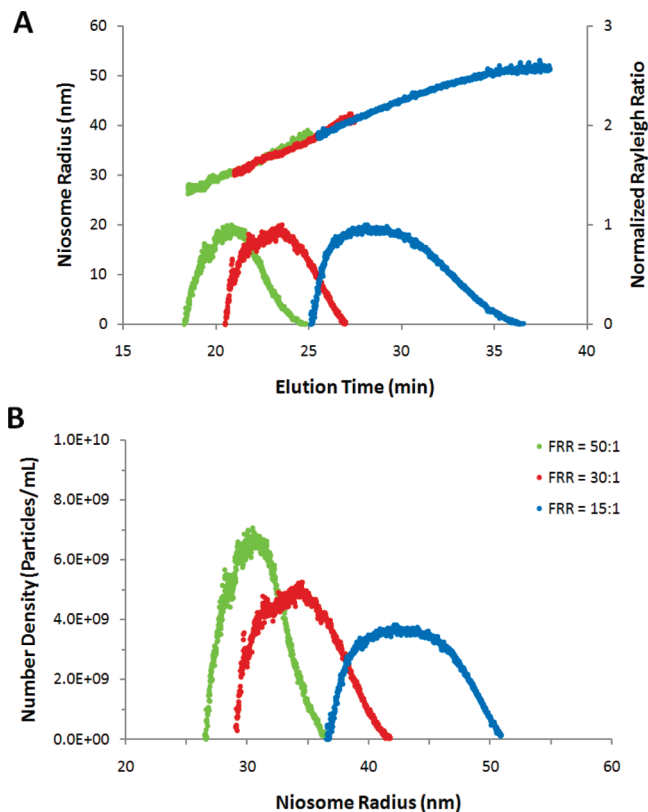


Figure 3. Niosomes assembled by microfluidic hydrodynamic focusing at various FRR were analyzed by asymmetric flow-field flow fractionation (AF⁴), in conjunction with multiangle laser light scattering (MALLS). The general principle of AF⁴ is to apply a high cross-flow to initially focus niosomes against a membrane, and then a quasi-parabolic flow is applied perpendicularly to elute niosomes with regard to size. (A) Smaller niosomes formed at higher FRR eluted before larger niosomes formed at lower FRR. (B) The angular scattering function was then analyzed by Astra V software to obtain mean niosome sizes and size distributions. The size distributions were normalized to the same total particle count. Data presented are 95% confidence of size interval ($\approx \pm 2\sigma$ size distribution from mean radius).

solid at $25\ ^\circ\text{C}$, with a transition temperature of $45\ ^\circ\text{C}$. When Span 60 came in contact with the PBS during focusing, it could have become aggregated because of its low solubility in water at $25\ ^\circ\text{C}$ (i.e., $25\ ^\circ\text{C} \ll T_c$). This explanation agrees with conventional bulk methods using Span 60, in which the surfactant and hydration buffer mixture requires heating above $50\ ^\circ\text{C}$ for niosome preparation.^{2,29,31} Since temperature control is beyond the scope of this study, it will be investigated in a future study. Therefore, Span 60 was excluded from the niosome self-assembly investigation in both the silicon and the PDMS devices.

Increase in FRRs and Not Q_T Results in Smaller Niosomes. In a microfluidic format, the volumetric flow rates can affect the outcome of the experiment. Therefore, various FRRs (flow rate ratio of PBS to IPA) and Q_T (total volumetric flow rate) were investigated to see whether a change in either parameter will affect the sizes of the assembled niosomes. An example of the

(29) Manosroi, A.; Wongtrakul, P.; Manosroi, J.; Sakai, H.; Sugawara, F.; Yuasa, M.; Abe, M. *Colloids Surf., B* **2003**, *30*, 129.

(30) Kato, K.; Walde, P.; Koine, N.; Ichikawa, S.; Ishikawa, T.; Nagahama, R.; Ishihara, T.; Tsujii, T.; Shudou, M.; Omokawa, Y.; Kuroiwa, T. *Langmuir* **2008**, *24*, 10762.

(31) Junyaprasert, V. B.; Teeranachaideekul, V.; Supaperm, T. *AAPS PharmSciTech* **2008**, *9*, 851.

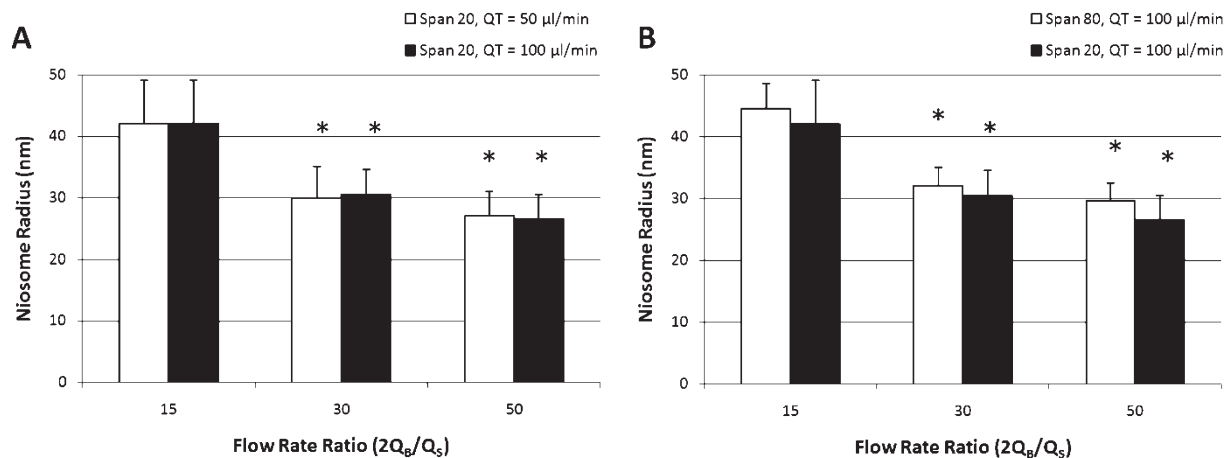


Figure 4. (A) Varying FRR and Q_T (total volumetric flow rate) were tested with Span 20 mixture for niosome self-assembly in the silicon device. An increase in FRR from 15 to 50 resulted in a decrease in niosome radius from 42 ± 7 to 27 ± 4 nm. Change in Q_T from 50 to $100 \mu\text{L}/\text{min}$, however, did not have any significant effects on the niosome size. (B) Span 80 mixture was also tested and found to assemble into similar sized niosomes as Span 20 mixture. At FRR of 50, Span 80 niosomes measured 30 ± 3 nm in radius, in comparison to 27 ± 4 nm of Span 20 niosomes. Note that the bars denote $\pm 1\sigma$ size distribution from mean radius ($*p < 0.05$ for both Span 20 and Span 80 niosomes, $n = 2-4$).

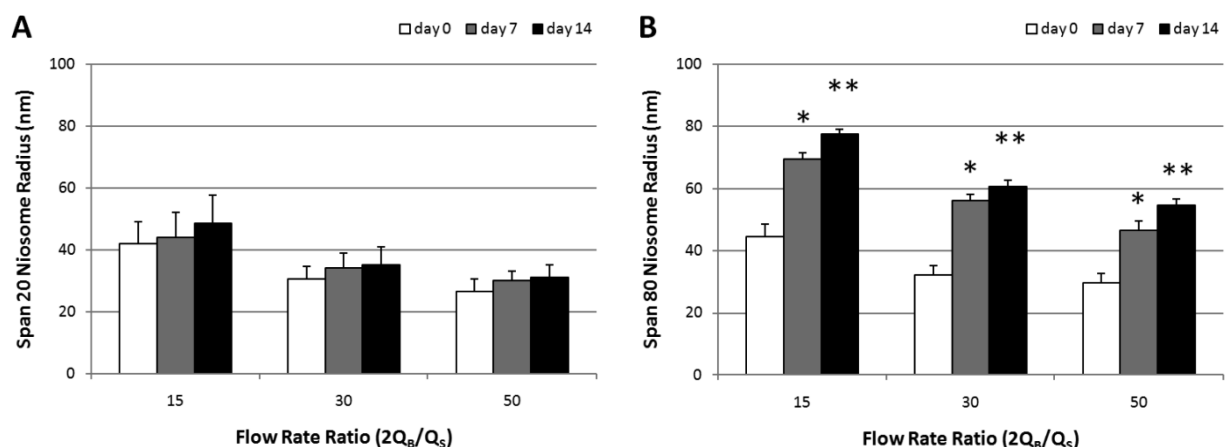


Figure 5. Niosomes collected from the silicon device at $Q_T = 100 \mu\text{L}/\text{min}$ were stored at 25°C and tracked over a 2-week study for (A) Span 20 niosomes and (B) Span 80 niosomes. Span 20 niosomes maintained similar size during storage in PBS, while Span 80 niosomes showed ≈ 1.8 -fold increase in radius compared to day 0. At FRR of 50, Span 80 niosomes measured initially at 30 ± 3 nm in radius but then increased to 55 ± 2 nm by the end of 14 days. Note that the bars denote $\pm 1\sigma$ size distribution from mean radius ($*p < 0.02$ for day 7 and $**p < 0.01$ for day 14 for Span 80 niosomes, $n = 2-4$).

niosome size and size distribution analysis from asymmetric flow-field flow fractionation (AF⁴), in conjunction with multiangle laser light scattering (MALLS), is presented in Figure 3. Using the silicon device, an increase in FRR from 15 to 50 resulted in a decrease in Span 20 niosome radius from 42 ± 7 to 27 ± 4 nm (Figure 4A). This correlation is consistent with our previous studies of liposome formation^{18,19} and can be explained by the shorter diffusive mixing time for niosome self-assembly at higher FRRs. The predicted diffusive mixing times from eq 1 are 1.8 ms for FRR of 15, 0.5 ms for FRR of 30, and 0.2 ms for FRR of 50. Using a Student's *t* test, the *p* values were calculated and confirmed that the niosome size differences seen between each test group and FRR of 15 was statistically significant. FRRs higher than 50 was not investigated because the IPA stream became unstable and started fluctuating during the sample collection interval. As for the affects of various Q_T on niosome self-assembly, $Q_T = 50$ and $100 \mu\text{L}/\text{min}$ were tested, and no significant difference was found with the sizes of the assembled niosomes (also Figure 4A). This result demonstrates that the mixing time of surfactant/IPA and PBS, and not the mixing

volume of the two liquids, is the more critical factor for niosome self-assembly using microfluidic hydrodynamic focusing.

Shorter and Saturated Alkyl Chain for Smaller and More Stable Niosomes. When comparing niosomes assembled from different Span mixtures, Span 20 niosomes were similar in size compared with Span 80 niosomes (Figure 4B). At FRR of 50, Span 20 niosomes measured 27 ± 4 nm in radius, while Span 80 niosomes measured 30 ± 3 nm. However, after storage at 25°C , there was an evident size difference between the two types of niosomes (Figure 5). Niosomes assembled from Span 20 showed a minimal ≈ 1.2 -fold increase in size after 2 weeks in PBS. Niosomes assembled from Span 80, in contrast, had ≈ 1.6 -fold increase after the first week and a total of ≈ 1.8 -fold increase by the end of the 2 weeks. The *p* values were calculated and confirmed that the niosome size increases seen in Span 80 were statistically significant. The difference in size stability between the two types of niosomes can be attributed to the chemical structures of the two Spans. Span 20 consists of an alkyl chain that is fully saturated, whereas Span 80 consists of a chain with a monounsaturations at C₉. The single bonds in Span 20 mean that the alkyl chain can

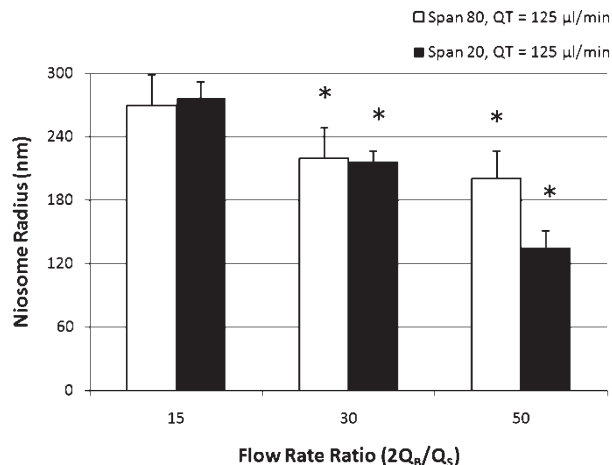


Figure 6. The 400 μm wide PDMS microchannel produced larger niosomes than the 65 μm wide silicon microchannel. At FRR of 50, Span 20 niosomes measured 136 ± 16 nm in radius for the PDMS device and 27 ± 4 nm for the silicon device. However, consistent with the silicon device, an increase in FRR in the PDMS device led to a decrease in niosome size. $Q_T = 125 \mu\text{L}/\text{min}$ was tested in the PDMS device in order to maintain similar volumetric flux as $50 \mu\text{L}/\text{min}$ in the silicon device. Note that the bars denote $\pm 1\sigma$ size distribution from mean radius (* $p < 0.05$ for both Span 20 and Span 80 niosomes, $n = 2-4$).

pack tightly, resulting in a rigid membrane for the assembled niosome. Meanwhile, the double bond in Span 80 does not allow rotation and produces a different bond angle in the alkyl chain, which prevents tight packing of the niosome membrane.^{32,33} This difference in the membrane packing means that the membranes for the Span 80 niosomes were more likely to swell than the membranes of the Span 20 niosomes.³⁴ It is also possible that Span 80 niosomes became larger because their longer alkyl chains were more energetically favored at reduced surface curvature.³⁵ Regardless of the cause, conventional bulk method preparation of niosomes also documented such an increase in Span 80 niosome size over time.³⁰ In summary, Span 20 mixture at FRR of 50 assembled into the smallest and most stable niosomes in the silicon device.

Wider Microchannel Geometry Leads to Larger Niosomes. Microchannel geometry is also another parameter that can affect the sizes of the assembled niosomes. Given the same flow conditions and at the same FRR, a wider microchannel produces a wider focusing width (Figure 2D), which can increase the diffuse mixing time as described by eq 1 and allow the surfactant mixture to self-assemble into larger niosomes. Indeed, the 400 μm wide PDMS microchannel produced niosomes of ≈ 300 nm in radius, whereas the 65 μm wide silicon channel produced niosomes of ≈ 50 nm in radius. The increase in the width of the PDMS microchannel geometry increased the predicted diffuse mixing time from 1.8 to 69.4 ms at FRR of 15. Nevertheless, the same correlation for FRR to niosome size was true for niosomes assembled in the PDMS device (Figure 6), with higher FRRs leading to smaller niosomes. Based on the p values, the niosome size differences seen in the higher FRRs were statistically significant compared to FRR of 15. The range of Q_T was

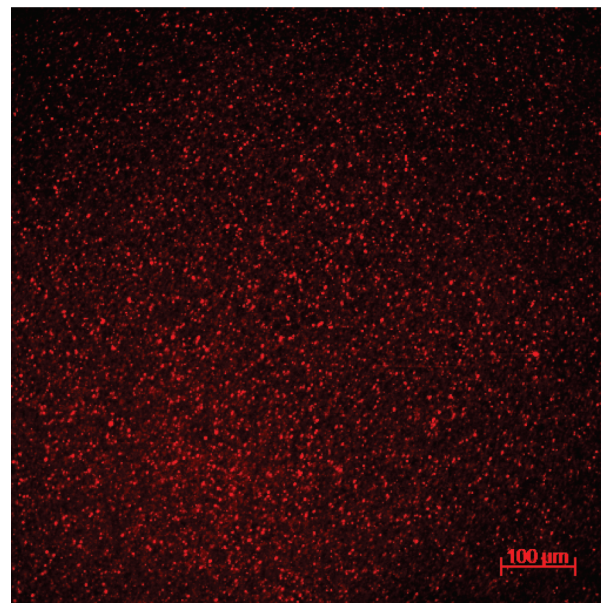


Figure 7. Niosomes assembled in the PDMS device at FRR of 15 were stained with DiIC₁₈(3), to confirm the presence of self-assembled membranes. The membrane intercalating dye became highly fluorescent once it was inserted into the intact niosome membranes; the fluorescence background of the dye dissolved in water was minimal. Note that fluorescence spot size does not correspond to actual vesicle size, since niosomes in our sample were smaller than the accessible optical resolution.

restricted to $125 \mu\text{L}/\text{min}$ (having the same volumetric flux as $50 \mu\text{L}/\text{min}$ in the silicon device) due to limitations of the PDMS device, which will be discussed in the next section. However, niosomes assembled in the PDMS device had intact self-assembled membranes, as demonstrated using a membrane intercalating dye DiIC₁₈(3). The quantum yield of this lipophilic dye increases dramatically once it intercalates into an intact membrane; the fluorescence background of the dye dissolved in water is minimal.^{36,37} The intensively fluorescent image of the stained niosomes is shown in Figure 7.

Considerations for Hydrodynamic Focusing in PDMS.

The PDMS device was tested in this study because it is more accessible to biological laboratories than the silicon device (i.e., without the need of a cleanroom setting). However, PDMS is a compliant polymer. High pressures from high volumetric flow rates can cause deformation of the top wall of the PDMS microchannel (i.e., height), whereas the other three channel walls are rigid since they are bonded to the glass substrate. As the deformation becomes substantial, it can affect the flow profile inside the microchannel and subsequently the ability to maintain a consistent focusing. Since deformation is proportional to the pressure inside the microchannel, we must initially calculate the pressure by using the following equation derived in Gervais et al.:³⁸

$$Q_T = \frac{h^4 E}{48\alpha\mu(L-z)} \left[\left(1 + \alpha \frac{p(z)W}{Eh} \right)^4 - 1 \right] \quad (3)$$

where Q_T is the total volumetric flow rate, h is the initial height of the channel, E is the Young's modulus of the channel walls (2 MPa

(32) Alberts, B.; Johnson, A.; Lewis, J.; Raff, M.; Roberts, K.; Walter, P. *Molecular Biology of the Cell*, 5th ed.; Garland Science: Oxford, 2007.

(33) Oxtoby, D. W.; Campion, A.; Gillis, H. P. *Principles of Modern Chemistry*, 6th ed.; Brooks Cole: Pacific Grove, CA, 2007.

(34) Rawicz, W.; Olbrich, K. C.; McIntosh, T.; Needham, D.; Evans, E. *Biophys. J.* **2000**, *79*, 328.

(35) Korreman, S. S.; Posselt, D. *Eur. Phys. J.* **2000**, *1*, 87.

(36) Axelrod, D. *Biophys. J.* **1979**, *26*, 557.

(37) Ladha, S. J. *J. Membr. Biol.* **1998**, *165*, 1.

(38) Gervais, T.; El-Ali, J.; Gunther, A.; Jensen, K. F. *Lab Chip* **2006**, *6*, 500.

for PDMS), α is a proportionality constant depending on the channel properties, μ is the viscosity of the fluid being pumped, L is the total length of channel plus the outlet tubing, z is the position of interest in the channel, $p(z)$ is the pressure at the position of interest, and W is the width of the channel. For a PDMS microchannel of similar dimensions to those in this study, α was measured by Hardy et al. to be 0.48.³⁹ We, therefore, obtained pressure values ranging from 33 to 24 kPa throughout the entire length of the microchannel for $Q_T = 125 \mu\text{L}/\text{min}$.

In shallow channels where $W \gg h$ and along with other simplifications,³⁸ the maximum change in channel height can be expressed as

$$\Delta h_{\text{max}} = C_1 \frac{pW}{E} \quad (4)$$

where Δh is the maximum change of height, p is the pressure at the point of deformation, and $c_1 = 3/2\alpha$. Note that the assumption here is that the top wall of the channel is deforming in a parabolic shape and that maximum deformation is occurring at the center of the microchannel. Using the pressure values previously calculated and eq 4, a maximum deformation of $4.7 \mu\text{m}$ at the beginning of the microchannel and a $3.4 \mu\text{m}$ deformation near the end of the channel were expected, corresponding to +8% and +6% vertical deformation, respectively. At $Q_T = 250 \mu\text{L}/\text{min}$, deformation of PDMS channel height was calculated to be +16% (greater than our tolerance of +10%) and produced a visible distortion of the PDMS microchannel. Thus, that particular volumetric flow rate was excluded from this study.

Another concern for using PDMS in microfluidics is the fact that the hydrophobic polymer is porous and will swell when overexposed to incompatible solvents. According to Lee et al.,⁴⁰ the solvents used in this study (i.e., IPA and PBS) have minimal swelling of PDMS before and after solvent exposure. PBS made with deionized water is most compatible, with a 1.00 swelling ratio (i.e., 0% swelling) of PDMS, whereas surfactants in IPA are somewhat compatible, with a 1.09 swelling ratio. It was also noted by the authors that these values were obtained after 24 h soaking of PDMS in each solvent and that pressure-driven flow of solvents through PDMS microchannels actually had minimal swelling effects relative to soaking.⁴⁰ However, it is important to note that other popular solvents typically used for bulk niosome preparation (e.g., chloroform, ether, methylene chloride) have substantial PDMS swelling ratios of > 1.20 and are thus not suitable for use in PDMS microfluidics. In short, the conditions we tested for niosome self-assembly in the PDMS device were compatible for the compliant polymer microchannel, with a maximum +8% channel height deformation from fluid flow as well as minimal swelling from the solvents used.

Comparisons with Bulk Method Niosome Preparation.

There are two popular bulk methods for niosome preparation in the laboratory: film hydration and alcohol injection. After production, niosomes can also be subjected to postprocessing steps to reduce the size and size distribution (i.e., extrusion or sonication). In the film hydration method, the surfactant mixture is initially dissolved in chloroform, evaporated to a dry film, and rehydrated with buffer. The solution is then gently shaken for several hours to produce the niosomes. Niosomes prepared by this method are generally quite large in size, ranging from 500 nm to $2 \mu\text{m}$ in radius.^{1,2,29} For the alcohol injection method, the surfactant mixture is dissolved in ethanol and slowly injected into

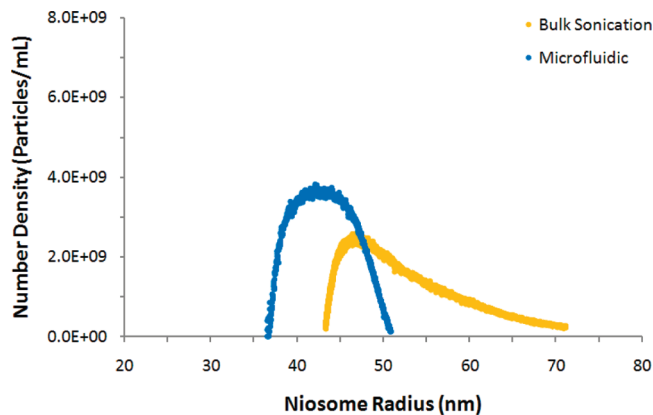


Figure 8. Niosomes prepared by the microfluidic method were smaller in size and $\approx 40\%$ narrower in size distribution, compared to niosomes prepared by the bulk method. Both methods utilized a PBS to IPA ratio of 15:1. The size distributions were normalized to the same total particle count. Data presented are 95% confidence of size interval ($\approx \pm 2\sigma$ size distribution from mean radius).

Table 2. Polydispersity Indices for Niosomes Prepared by Microfluidic Method

	Bulk	PI ^a	Silicon	FRR ^b	PI ^a	PDMS	FRR ^b	PI ^a
Span 20	1.24	Span 20	15	1.16	Span 20	15	1.03	1.03
			30	1.08		30	1.03	
			50	1.04		50	1.03	
Span 80	1.07	Span 80	15	1.02	Span 80	15	1.03	1.05
			30	1.02		30	1.05	
			50	1.02		50	1.04	

^a Polydispersity index. ^b Flow rate ratio.

a buffer to form the niosomes. This method can typically yield niosomes of 150 nm to $1 \mu\text{m}$ in radius,^{1,41,42} with a size distribution of $\approx \pm 40$ nm for the smallest niosomes. Further processing, such as extrusion through a membrane or sonication with a probe tip, can result in niosomes < 150 nm in radius.^{1,41} However, there were concerns that such postprocessing methods can affect the morphology of the niosomes.^{1,4}

With the new microfluidic method, we can rapidly prepare niosomes as small as 27 ± 4 nm in radius using the silicon device and 136 ± 16 nm in radius using the PDMS device. It is expected that reduction of the microchannel dimensions in the PDMS device will allow for the assembly of even smaller niosomes than the current reported size. The achievable niosome size ranges from the microfluidic method are much smaller than those of conventional bulk methods, without additional postprocessing steps. The size distribution of the niosomes obtained is also reduced by $\approx 40\%$ (Figure 8), given the same PBS to IPA ratio of 15:1. The polydispersity index (PI) was calculated from the Astra V software. The index is calculated as the second moment average radius (R_w) divided by the average radius (R_n) to indicate the distribution of niosome sizes in a batch of niosomes:

$$\text{PI} = \frac{R_w}{R_n} \quad (5a)$$

$$R_w = \frac{\sum R_i^2 N_i}{\sum R_i N_i}, \quad R_n = \frac{\sum R_i N_i}{\sum N_i} \quad (5b)$$

(41) Baillie, A. J.; Coombs, G. H.; Dolan, T. F. *J. Pharm. Pharmacol.* **1986**, *38*, 502.

(42) Rogerson, A.; Cummings, J.; Willmott, N.; Florence, A. T. *J. Pharm. Pharmacol.* **1988**, *40*, 337.

(39) Hardy, B. S.; Uechi, K.; Zhen, J.; Kavehpour, H. P. *Lab Chip* **2009**, *9*, 935.

(40) Lee, J. N.; Park, C.; Whitesides, G. M. *Anal. Chem.* **2003**, *75*, 6544.

where N_i is the number of niosomes with radius R_i . The PI has a value always > 1 because R_w is always greater than R_n . When niosome sizes are almost uniform, the PI approaches the value of 1. PI values obtained from this study are listed in Table 2. With the bulk method, the PI value of Span 20 was much greater than that of Span 80 ($1.24 > 1.07$). However, this difference was minimized for niosomes prepared by the microfluidic method (example: $1.04 > 1.02$ at FRR of 50 in the silicon microchannel). In addition, niosomes prepared by the microfluidic method all had indices near the value of 1, which are considered monodisperse. Therefore, we can obtain nanoscaled niosomes with more monodisperse size distributions in our microfluidic format than conventional bulk methods.

4. Conclusions

We have demonstrated in this study that controlled self-assembly of niosomes, a synthetic and inexpensive alternative to liposomes, can be achieved by diffusive mixing of two *miscible* fluids (i.e., alcohol and water) using microfluidic hydrodynamic focusing. We found several parameters that can greatly affect the sizes of the assembled niosomes. An increase in FRR decreased diffusive mixing time and subsequently produced smaller niosomes, while a wider microchannel geometry led to an increase in diffusive mixing time and larger niosomes. With respect to the

surfactants tested, Span 20 with saturated and shorter C_{12} alkyl chain assembled into the smallest and most stable niosomes. Furthermore, both the silicon metal microchannels and the PDMS polymer microchannels (which are more accessible to biological laboratories) were capable of achieving hydrodynamic focusing for on-chip assembly of niosomes.

Because niosomes prepared by the microfluidic method were nanoscaled in size and more monodisperse in size distribution than conventional bulk methods, they can potentially provide consistent encapsulation of molecules for more reliable clinical therapeutics and imaging. For future studies, we hope to investigate the encapsulation efficiency of such niosomes for clinical applications. We anticipate that a quick postmicrofluidic evaporation step can remove the minimal solvent in the niosome solutions. If *in vivo* toxicity is a concern, ethanol can also be used as an alternative solvent for niosome preparation. This work suggests that microfluidics may facilitate the development and optimization of biomimetic colloidal systems for nanomedicine applications.

Acknowledgment. C.T.L. acknowledges the financial support from the NIST/NRC Postdoctoral Research Program, the helpful discussions with Dr. Jason Kralj, and the microscopy assistance provided by Dr. Jennifer Hong. The authors also thank Dr. Laura Hermida for the introduction to niosomes.